Extracellular vesicles synchronize cellular phenotypes of differentiating cells

AUTHOR(S):

Minakawa, Tomohiro; Matoba, Tetsuya; Ishidate, Fumiyoshi; Fujiwara, Takahiro K.; Takehana, Sho; Tabata, Yasuhiko; Yamashita, Jun K.

CITATION:

Minakawa, Tomohiro ...[et al]. Extracellular vesicles synchronize cellular phenotypes of differentiating cells. Journal of Extracellular Vesicles 2021, 10(11): e12147.

ISSUE DATE:

2021-09

URL:

http://hdl.handle.net/2433/265343

Received: 28 October 2020 | Revised: 26 August 2021 | Accepted: 5 September 2021

DOI: 10.1002/jev2.12147

RESEARCH ARTICLE

Extracellular vesicles synchronize cellular phenotypes of differentiating cells

Tomohiro Minakawa[1] | **Tetsuya Matoba**[2] | **Fumiyoshi Ishidate**[3] | **Takahiro K. Fujiwara**[3] | **Sho Takehana**[4] | **Yasuhiko Tabata**[4] | **Jun K. Yamashita**[1]

[1] Department of Cell Growth and Differentiation, Centre for iPS Cell Research and Application (CiRA), Kyoto University, Kyoto, Japan

[2] Department of Cardiovascular Medicine, Kyushu University Graduate School of Medical Sciences, Fukuoka, Japan

[3] iCeMS Analysis Centre, Institute for Integrated Cell-Material Sciences (WPI-iCeMS), Kyoto University Institute for Advanced StudyKyoto University, Kyoto, Japan

[4] Laboratory of Biomaterials, Institute for Frontier Life and Medical Sciences, Kyoto University, Kyoto, Japan

Correspondence
Jun K. Yamashita, Department of Cell Growth and Differentiation, Centre for iPS Cell Research and Application (CiRA), Kyoto University, Kyoto 606–8507, Japan.
Email: juny@cira.kyoto-u.ac.jp

Funding information
JST CREST, Grant/Award Number: JPMJCR17H5

Abstract

During embryonic development, cells differentiate in a coordinated manner, aligning their fate decisions and differentiation stages with those of surrounding cells. However, little is known about the mechanisms that regulate this synchrony. Here we show that cells in close proximity synchronize their differentiation stages and cellular phenotypes with each other via extracellular vesicle (EV)-mediated cellular communication. We previously established a mouse embryonic stem cell (ESC) line harbouring an inducible constitutively active protein kinase A (CA-PKA) gene and found that the ESCs rapidly differentiated into mesoderm after PKA activation. In the present study, we performed a co-culture of Control-ESCs and PKA-ESCs, finding that both ESC types rapidly differentiated in synchrony even when PKA was activated only in PKA-ESCs, a phenomenon we named 'Phenotypic Synchrony of Cells (PSyC)'. We further demonstrated PSyC was mediated by EVs containing miR-132. PKA-ESC-derived EVs and miR-132-containing artificial nano-vesicles similarly enhanced mesoderm and cardiomyocyte differentiation in ESCs and ex vivo embryos, respectively. PSyC is a new form of cell-cell communication mediated by the EV regulation of neighbouring cells and could be broadly involved in tissue development and homeostasis.

KEYWORDS
differentiation, embryos, miR-132, nanoparticles, stem cells, synchronization

1 | INTRODUCTION

Embryonic development is an extremely fine-tuned and orchestrated process. Individual cells must differentiate in a coordinated manner to form normal tissues. Numerous studies have investigated signalling pathways and gene regulation mechanisms during development (Arnold & Robertson, 2009). However, how each cell synchronizes its differentiation with surrounding cells during development is largely unknown. Limited experimental systems have hampered detailed studies on the synchronization.

Embryonic stem cells (ESCs) are derived from the inner cell mass (ICM) of early blastocysts and can differentiate from the pluripotent state into all three germ layers in vitro, making them one of the most powerful tools for studying the cell differentiation process (Evans & Kaufman, 1981; Martin, 1981; Thomson et al., 1998). We previously generated a mouse ESC line, PKA-ESCs, in which protein kinase A (PKA) is constitutively activated by the depletion of doxycycline (Dox-) (Figure 1a) (Yamamizu et al., 2009). PKA activation with Dox- during ESC differentiation in two-dimensional (2D) culture accelerates the appearance of the three germ layers, especially mesoderm cells through a signal-epigenetic linkage (Minakawa et al., 2020). This cell line system is amenable to manipulating the cell differentiation speed only in PKA-ESCs independent of other cell lines; that is, different differentiation speeds can be intentionally generated between activated PKA-ESCs and surrounding ESCs.

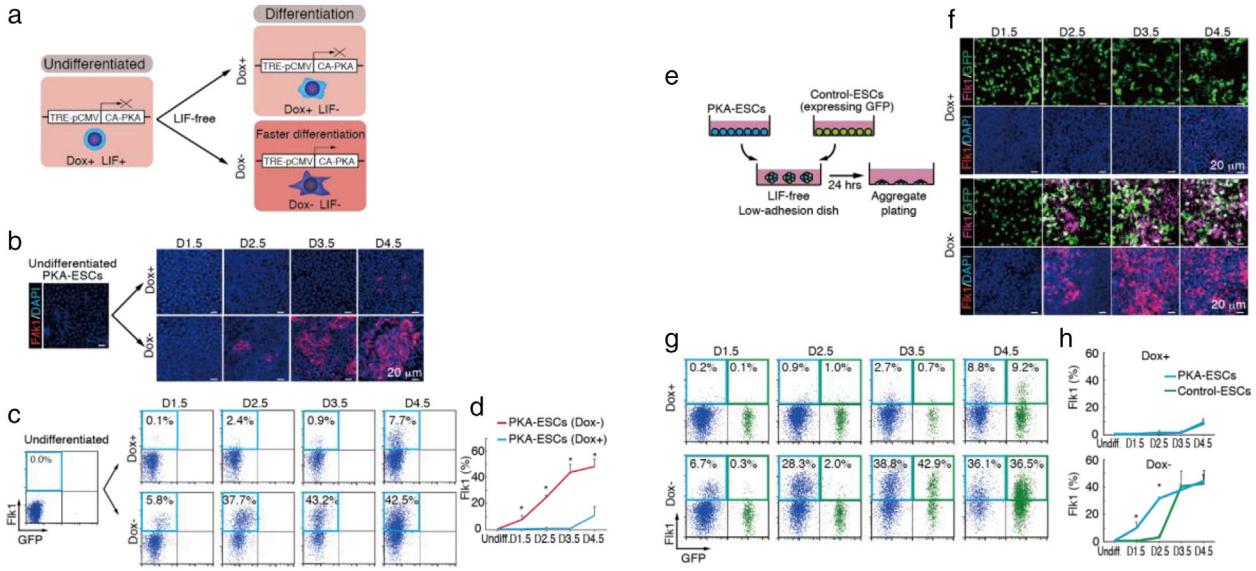

FIGURE 1 Mouse ESCs synchronize their timing of differentiation with each other. (a) Experimental system of PKA activation. PKA-ESCs express a constitutively active form of PKA (CA-PKA) via a Dox-regulated expression system. To maintain the undifferentiated state, PKA-ESCs were cultured in the presence of LIF and Dox. LIF is excluded for the induction of differentiation. PKA-ESCs differentiate faster in the absence of Dox (Dox-) than presence (Dox+). (b) Immunostaining for Flk1 during the differentiation of PKA-ESCs. (c) FACS analysis for Flk1 appearance on PKA-ESCs. (d) Percentage of PKA-ESCs expressing Flk1 by FACS analysis. Data were analysed using the Mann-Whitney U test. Under Dox- conditions, PKA-ESCs showed earlier and significantly more Flk1$^+$ cells. $^*P < 0.05$ relative to PKA-ESCs (Dox+). (e) Schematic diagram of the chimeric aggregate co-culture differentiation system. PKA-ESCs and Control-ESCs were seeded in low adhesion dishes at a 3:1 ratio to create chimeric aggregates, and differentiation induction was initiated by the depletion of LIF. 24 h later, aggregates were replated on normal plates and attached around 12 h later. (f) Immunostaining for Flk1 during the differentiation of PKA-ESC and Control-ESC chimeric aggregates. The number of Flk1$^+$ Control-ESCs in chimeric aggregates (white) increased in Dox- condition. (G) FACS analysis of the Flk1 appearance on chimeric aggregates. Under Dox- condition, Flk1$^+$ cells in the PKA-ESC population (blue) appear earlier, but by D3.5, the percentage of Flk1$^+$ cells in the Control-ESC population (green) is the same as in the PKA-ESC population. (H) Percentage of chimeric aggregates expressing Flk1 during differentiation. Data represent means ± S.D and were analysed using the Mann-Whitney U test. $^*P < 0.05$, relative to Control-ESCs

In the present study, we performed chimeric aggregate cultures of PKA-ESCs and a control ESC line expressing GFP (Control-ESCs). This experimental system enabled us to intentionally generate different differentiation speeds between two ESC populations in a 3D condition that resembles embryonic development, because the differentiation is specifically accelerated only in PKA-ESCs by Dox-. With the use of this unique system, we succeeded in revealing a new phenomenon in which slower differentiating cells synchronize their phenotype with that of faster differentiating cells to reach the same differentiation stage. We name this phenomenon, 'Phenotypic Synchrony of Cells (PSyC)'. We also investigated the molecular machinery that regulates PSyC and identified extracellular vesicles (EVs) and their micro RNA (miRNA) content as responsible. PSyC in chimeric cellular aggregates was abrogated by treatment with EV inhibitors. EVs from activated PKA-ESCs promoted the mesodermal differentiation of Control-ESCs and promoted the mesodermal differentiation and even cardiomyocyte differentiation of mouse embryos in ex vivo culture. In addition, among the molecules specifically increased in EVs from PKA-activated ESCs, we identified miR-132 as a functional molecule that can reconstitute the PKA activation and enhanced differentiation of mesoderm lineages in EV-recipient cells. Moreover, a similar cardiomyocyte induction was reproduced by adding artificial nano-particles containing miR-132 to ex vivo mouse embryo culture.

Cell-cell communication via EVs in various tissues has been reported (Yáñez-Mó et al., 2015). PSyC offers another mode of this communication and a phenotypic regulation through EVs mainly between cells in close proximity. Our findings provide new understandings about intercellular communication and possible novel strategies towards regenerative medicine by manipulating cell fates through this novel EV function.

2 | MATERIALS AND METHODS

2.1 | ESC lines

PKA-ESC: A mouse ESC line carrying a tetracycline-regulatable constitutively active form of the PKA (CA-PKA) gene (Yamamizu et al., 2009). It was generated as described previously.

EStTA5-4: A mouse ESC line expressing the tetracycline-transactivator protein and containing the puromycin resistance gene (Era & Witte, 2000). It was a kind gift from Dr. Takumi Era (Kumamoto University).

Control-ESC (GFP-ESC): A mouse ESC line carrying a ubiquitous promoter-driven EGFP gene. It was generated by introducing a plasmid carrying the EGFP gene under the control of the CAG promoter in EStTA5-4 cells using the Amaxa Mouse ES cells Nucleofector Kit (VPH-1001, Lonza).

ES-D3 cells (D3-ESCs) (Yurugi-Konayashi et al., 2006): Another control ESC line used in the experiments.

To generate seven mouse ESC lines carrying tetracycline-regulatable miRNAs and GFP, piggyBac vectors carrying primary miRNA genes under the tetracycline response element (TRE) promoter and a transposon vector were introduced to EStTA5-4 using lipofectamine LTX Reagent (15338500, Thermo Fisher Science). The copy number of the miRNAs in EVs derived from these cell lines was measured by droplet digital polymerase chain reaction (ddPCR) (Chevillet et al., 2014).

CD81-tdTomato PKA-ESC: A plasmid expressing tdTomato-CD81 fusion protein was introduced into PKA-ESC using the Amaxa Mouse ES cells Nucleofector Kit.

An miR-132 knockout (KO) PKA-ESC line was generated by replacing the genome region of miR-132 with single-strand oligodeoxynucleaotides (ssODNs) including a minimal promoter and HiBit (Promega). The ssODNs (synthesized by Integrated DNA Technologies, Coralville, USA) and pX330 plasmids expressing Cas9 and a sgRNA targeting the miR-132 locus were introduced into PKA-ESCs using lipofectamine LTX Reagent.

Cells were selected by detecting HiBit protein using the Nano Glo HiBiT Lytic Detection System (N3030, Promega). pX330 was a kind gift from Dr. Feng Zhang (Massachusetts Institute of Technology).

2.2 | ddPCR

MiRNAs were extracted from cells or EV samples using the miRNeasy Mini Kit (217004, QIAGEN). cDNA was synthesized using the mir-X miRNA First-Strand Synthesis Kit (63815, Takara, Japan). An Automated Droplet Generator QX200 ddPCR system (Bio-Rad) was used for all ddPCR of synthesized cDNA.

2.3 | Plasmid construction

Primary miRNA genes were amplified by PCR from the genomic DNA of mouse ESCs, and the multi-miRNA (multi-miR) sequence was synthesized by GENEWIZ (New Jersey, USA). These sequences were cloned into the pENTR plasmid vector followed by recombination with a piggyBac vector (Woltjen et al., 2009) using Gateway LR Clonase II Enzyme Mix (11791-020, Thermo Fisher Scientific). The piggyBac vector and transposon vector were kind gifts from Dr. Knut Woltjen (CiRA, Kyoto University).

2.4 | Cell culture and differentiation

ESC lines were maintained in Glasgow Minimum Essential Medium (GMEM; 11710-035, Thermo Fisher Scientific) containing 10% KnockOut Serum Replacement (KSR; 10828-028, Thermo Fisher Scientific), 1% fetal bovine serum (FBS; SAFC Biosciences, USA), 2000 units/ml leukaemia inhibitory factor (LIF; Merck Millipore), 1 mM sodium pyruvate (Sigma-Aldrich), 1% MEM Non-Essential Amino Acids (NEAA; 11140-050, Thermo Fisher Scientific), 50 U/ml penicillin (Meiji Seika Pharma, Japan), 50 μg/ml streptomycin (Meiji Seika Pharma, Japan) and 0.1 mM 2-mercaptoethanol (2-ME; 21985-023, Thermo Fisher Scientific). For the maintenance of PKA-ESCs, 1 μg/ml Dox was added.

Differentiation was induced in MEM alpha (11900-024, Thermo Fisher Scientific) containing 10% FBS (10437-028, Thermo Fisher Scientific), 2.2 μg/ml $NaHCO_3$ (09655-25, Nacalai Tesque, Japan), 50 U/ml penicillin, 50 μg/ml streptomycin and 0.1 mM 2-ME. In this study, we used FBS without EV-depletion because the culture condition is suitable for the stable ESC differentiation. We confirmed the negligible effects of EV-containing serum on our ESC differentiation. There was no effect on differentiation efficiency whether EV-depleted or non-depleted serum was used (Figures S1A and S1B). Addition of serum-derived EVs to the cells also had no effect on differentiation (Figures S1C and S1D).

To inhibit the secretion of EVs, aggregates were treated with manumycin A (BVT-0091, BioViotica) or GW4869 (13127, Cayman Chemical).

2.5 | Aggregate formation

ESC lines were seeded on a low adhesion dish, PrimeSurface Dish 35 mm (MS-9035X, Sumitomo Bakelite, Japan) or low-cell-adhesion 96-well plates with U-bottomed conical wells (9,000 cells per well, 100 ml; MS-9096U, Sumilon PrimeSurface plate,

Sumitomo Bakelite) using differentiation medium. After 24 h, floating aggregates were collected and plated on multi-well plates (Falcon). To make chimeric cell aggregates, ESC lines were mixed in ratios as indicated.

2.6 | FACS analysis

Cultured cells were harvested at day (D)1.5, D2.5, D3.5 and D4.5 during the differentiation, stained with combinations of allophycocyanin (APC)-conjugated anti-Flk1 mAb (AVAS12) (Kataoka et al., 1997) and phycoerythrin (PE)-conjugated anti-platelet-derived growth factor receptor α (PDGFRα) mAb (12-1401-81, eBioscience) and then subjected to analysis with a FACS Aria (Becton Dickinson) or CytoFLEX S (Beckman Coulter).

2.7 | Immunohistochemistry

Cultured cells were fixed in ice-cold 4% paraformaldehyde solution for 1 h, blocked in 2% skim milk (232100, Becton Dickinson) for 24 h at 4°C and incubated with primary antibodies for 24 h at 4°C.

The following primary antibodies were used: Flk1 (AVAS12, prepared in house, 1:500,000), PDGFRα (3174S, Cell Signalling Technology, 1:500), Oct4 (sc-5279, Santa Cruz Biotechnology, 1:200) and Nanog (RCAB002P, ReproCELL, Japan, 1:300).

After the primary antibody incubation, the cells were washed with phosphate buffered saline (PBS) three times and incubated with secondary antibodies conjugated to Alexa Fluor (Thermo Fisher Scientific, 1:500) for 24 h at 4°C. Nuclei were visualized with DAPI (4,6 diamidino-2-phenylindole; D3571, Thermo Fisher Scientific).

2.8 | RNA sequencing (RNA-seq) of miRNAs

For bulk RNA-seq, small RNA was extracted using a miRCURY RNA Isolation Kit (300110, EXIQON). We prepared sequencing libraries using the TruSeq Small RNA Library Prep Kit (illumina). The libraries were sequenced in the 50 cycle Single-Read mode of HiSeq2500. All sequence reads were extracted in FASTQ format using BCL2FASTQ Conversion Software 1.8.4 in the CASAVA 1.8.2 pipeline. The sequence reads were mapped to mm10 reference genes using MirDeep and normalized and quantified using RPKMforGenes, downloaded on 10 December 2012. Gene expression levels were represented by log2(RPKM+1).

2.9 | Western blotting

Isolated EVs and cells were washed with PBS, lysed with 10x RIPA buffer (9806S, Cell Signalling Technology) and incubated at room temperature for 1 h. The mixtures were centrifuged at 12,000 g for 5 min at 4°C. The supernatants were collected as protein extracts. 6x sample buffer solution without 2-ME (09500-64, Nacalai Tesque, Japan) was added to the extract, and the mixture was incubated at 95°C for 5 min. The samples were then centrifuged at 12,000 g for 5 min at 4°C to remove insoluble precipitates. Supernatants were subsequently loaded onto sodium dodecyl sulphate-polyacrylamide gel electrophoresis (SDS-PAGE) with the use of a gradient gel (E-T1020L, Atto, Japan), followed by electrophoretic transfer onto nitrocellulose membranes. We loaded an equal amount of protein per sample (3 or 30 μg) as determined by the BCA Protein Assay Kit (06385-00, Nacalai Tesque, Japan). After the blotting, the membranes were incubated for 1 h in blocking agent Blocking One (03953-95, Nacalai Tesque, Japan), then for 24 h with primary antibodies at 4°C. The Can Get Signal Immunoreaction Enhancer Solution Kit (NKB-101, Toyobo, Japan) was used as antibody diluent for the signal enhancement. Immunoreactivity was detected using an enhanced chemiluminescence kit, Immobilon Western (WBKLS0500, Merck Millipore). Signal intensities were calculated using ImageQuant TL Software (GE Healthcare Life Sciences).

2.10 | Capillary western blot (WES)

Cell lysates were processed with a NE-PER Nuclear and Cytoplasmic Extraction Kit (78835, Thermo Fisher Scientific) to separate cytoplasmic and nuclear fractions. Phosphorylated cyclic AMP response element-binding protein (pCREB), Spry1 and Rasa1 expression levels were measured using a WES device (Protein Simple).

2.11 | ELISA (Enzyme-Linked ImmunoSorbent Assay)

Total CREB and pCREB were quantified by ELISA (85-86153-11, Instant One ELISA CREB1, Thermo Fisher Scientific) in accordance with the manufacturer's instructions.

2.12 | RNA isolation, RT-PCR (reverse transcription PCR)

Total RNA was isolated from cultured cells using RNeasy (74104, QIAGEN). cDNA was synthesized using SuperScript III (11752-050, Thermo Fisher Scientific) following the manufacturer's instructions. Quantitative RT-PCR was performed using Power SYBR Green PCR Master Mix (4367659, Thermo Fisher Scientific) and the StepOnePlus system (Thermo Fisher Scientific). Values for each gene were normalized to the relative quantity of GAPDH mRNA in each sample.

2.13 | EV isolation

1.0×10^5 PKA-ESCs were seeded in 10-cm dishes with differentiation medium. After 2 days, the medium was changed to a fresh one. After a further 1.5–2.5 days of culture, the conditioned medium was collected and centrifuged at 2,000 g for 20 min at room temperature. The supernatant was collected and centrifuged at 12,000 g for 30 min at room temperature. To remove cellular debris and a clump of extracellular matrix, the supernatant was filtered through a 0.2 μm pore filter (Sartorius, Germany) Then the supernatant was ultra-centrifuged at 100,000 g for 60 min at 4°C. EVs were isolated as pellets.

For the in vitro EV-treatment experiments, EVs (approximately 1.0×10^{10} particles) were added to the cells based on qNano (IZON, UK) analysis. For the ex vivo EV treatment experiments, EVs (approximately 1.0×10^{10} particles) were added in four aliquots.

2.14 | Size distribution and particle concentration

EVs were resuspended in PBS, and the size and number of particles were analysed using qNano (Izon, Christchurch, New Zealand). The NP100 nanopore (Izon) was used for detecting particles, and the measuring system was calibrated using CPC100 calibration particles (Izon). Particles were measured at 47.0 mm stretch at 0.7 V.

2.15 | Transmission electron microscopy analysis

EVs were suspended in PBS (30 μg/ml), dropped (20 μl/drop) on the membrane side of a carbon-stabilized collodion-coated grid (400 mesh; Nisshin-EM, Japan) and left for 10 min at room temperature. The solution was removed with filtered paper and rinsed with distilled water. 1% solution of uranyl acetate dissolved in distilled water was applied to the grid, which was then left to sit for 1 min at room temperature. Then the reagent was removed with filtered paper and dried. The EVs were imaged with a transmission electron microscope (H-7650, Hitachi High-Technologies, Japan).

2.16 | Mice

Pregnant ICR mice on day 3.5 or day 6.5 were purchased from Japan SLC, Inc.

2.17 | Embryo ex vivo culture

E6.5 embryos were isolated by dissecting the uterus and decidua in Dulbecco's Modified Eagle's Medium (DMEM)/F12 (1:1)(11039-012, Thermo Fisher Scientific) with 5% FBS (SAFC Biosciences, USA). Isolated embryos were cultured on a 12 mm Transwell with a 0.4 μm pore (3460, Corning) for low-adhesion with 500 μl DMEM (21063-029, Thermo Fisher Scientific) containing 50% rat serum, 0.1 mM NEAA, 1 mM sodium pyruvate and 0.5 mM 2-ME. After 2 days of culture with or without EVs, the embryos were dissociated with 0.25% trypsin/ethylenediaminetetraacetic acid (EDTA) for 15–25 min at 37°C. The cells were then stained with PE-conjugated anti-PDGFRα mAb (12-1401-81, eBioscience) and subjected to analysis using a FACS Aria (Becton Dickinson).

E3.5 embryos were recovered by flushing uteri with KSOM medium (prepared in house). Embryos were collected into drops of M2 medium (M7167, Sigma-Aldrich). Zona pellucida were removed by brief exposure to acidic Tyrode's solution drops (T1788, Sigma-Aldrich). M2 medium drops and Tyrode's solution drops were covered with mineral oil (HiGROW OIL, Fuso Pharmaceutical Industries, Japan) and pre-equilibrated at 37°C with 5% CO_2. Zona-freed blastocysts were washed with in vitro culture medium (IVC1) (Advanced DMEM/F12 (12634-010, Thermo Fisher Scientific) containing 20% FBS and supplemented with 2 mM L-glutamine (25030-081, Thermo Fisher Scientific), penicillin (25 units/ml)/streptomycin (25 μg/ml), 1x Insulin-Transferrin-Selenium-Ethanolamine (ITS-X) (51500-056, Thermo Fisher Scientific), 8 nM β-estradiol (E8875, Sigma-Aldrich), 200 ng/ml progesterone (160-24511, Wako, Japan) and 25 μM N-acetyl-L-cysteine (A7250, Sigma-Aldrich)) to remove the mineral oil and

M2 medium and seeded on a μ-slide 8 well (80826, Ibidi, Germany) filled with pre-equilibrated IVC1 medium, as previously described (Bedzhov et al., 2014). Two or three days after the embryos were attached on the bottom of the plates, the medium was exchanged to chemically defined IVC2 medium (Advanced DMEM/F12 containing 30% KSR and supplemented with 2 mM L-glutamine, penicillin (25 units/ml)/streptomycin (25 μg/ml), 1x ITS-X, 8 nM β-estradiol, 200 ng/ml progesterone and 25 μM N-acetyl-L-cysteine). The embryo culture was performed at 37°C in 5% CO_2. The embryos were treated with EVs (approximately 2.5×10^9 particles) or polymer poly (DL-lactide-co-glycolide) (PLGA) nanoparticles every 2 days between day 2 and day 8. All animal experiments were performed in accordance with the guidelines for Animal Experiments of Kyoto University, which conform to the Guide for the Care and Use of Laboratory Animals in Japan.

2.18 | Preparation of PLGA nanoparticles

Biotinized PLGA with an average molecular weight of 20,000 Da and a copolymer ratio of lactide to glycolide of 75:25 (Nanosoft Polymers, NC, USA) was used as the matrix for the nanoparticles, and polyvinylalcohol (PVA-403, Kuraray, Japan) was used as the dispersing agent. PLGA nanoparticles incorporating a mirVana miRNA mimic hsa-mir 132–3p (4464066, Thermo Fisher Science) were prepared using an emulsion solvent diffusion method in RNAase-free water, as previously described (Kawashima et al., 1998). The sequences of human miR-132-3p and mouse miR-132-3p are identical. miR-132-PLGA contained 11.6% (w/w) miR-132. A sample of the nanoparticle suspension in distilled water was used to determine the particle size. The median diameter of miR-132-PLGA based on dynamic light scattering was 262 nm.

2.19 | Tracking miR-132 with molecular beacons (MB)

The MB sequence 5′-[Alexa647]-CGCGATC-GTAACAATCGAAAGCCACGGTT-GATCGCG-[Iowa Black RQ]-3′ was purchased from Integrated DNA Technologies, Inc. (USA). Cationized gelatin spheres (cGNS) for encapsulating the MB were prepared as previously reported (Murata et al., 2021). 50 μl cGNS (1 mg/ml) and 10 μl MB (100 μM) were mixed with 440 μl double distilled water (DDW), and the mixture was incubated for 15 min at room temperature in the dark and then centrifuged at 8,000 g for 15 min. The supernatant was removed, and the pellet (cGNS/MB) was resuspended in 100 μl distilled water.

1.0×10^5 PKA-ESCs were seeded in 10-cm dishes with differentiation medium. After 2 days, the cells were washed with PBS twice and then incubated with 5 ml Opti-MEM (31985-070, Thermo Fisher Science) and 100 μl of cGNS/MB solution at 37°C for 1–3 h. The cells were washed twice with PBS and cultured with differentiation medium. After 2 and 3 days, the conditioned medium was collected. EVs were collected from the conditioned medium by ultra-centrifugation and added to Control-ESCs.

2.20 | Statistical analysis

The significance of differences was evaluated using the Mann–Whitney U test for comparisons between two groups or by the Kruskal–Wallis test, followed by the Steel–Dwass test for multiple comparisons. $P > 0.05$ was considered not significant.

3 | RESULTS

3.1 | Mouse ESCs synchronize their stage of differentiation

In our previous differentiation condition (differentiation medium with serum) in 2D culture, mouse ESCs gave rise to $Flk1^+$ mesoderm cells at around 4 days of differentiation (D4) (Minakawa et al., 2020; Yamashita et al., 2000). In the present study, first we confirmed the differentiation speed of mouse ESCs in cell aggregates (Figure S2A). Similar to our recent report (Minakawa et al., 2020), activated PKA-ESCs (Dox-) in cell aggregates differentiated much more rapidly to $Flk1^+$ cells than did non-activated PKA-ESCs (Dox+) (Figure 1b). Quantitatively, we found fewer than 1% of total non-activated PKA-ESCs were $Flk1^+$ at D3.5, but more than 40% of activated PKA-ESCs were (Figures 1c and 1d). The appearance of a mesoderm population expressing another mesoderm marker, PDGFRα^+, was also enhanced upon PKA activation (Figures S2B, S2C and S2D). The differentiation speed of Control-ESCs was not affected by Dox exposure (Figures S2E-S2J). In both Dox+ and Dox-, the percentage of $Flk1^+$ cells in Control-ESCs was less than 10% at D3.5 (Figure S2E). We then created chimeric cell aggregates of PKA-ESCs and Control-ESCs (Figure 1e). In this co-culture system, PKA activation can generate different differentiation speeds between the two cell lines; that is, the differentiation is expected to be accelerated only in PKA-ESCs after PKA activation with Dox depletion. Surprisingly, however, in the chimeric aggregates, PKA activation in PKA-ESCs induced an earlier appearance of mesoderm cells not only in PKA-ESCs, but also in Control-ESCs at D3.5 at comparable levels (Figures 1f-1h). Immunostaining for Flk1 (Figure 1f) showed

that under Dox- condition, an earlier appearance of Flk1$^+$ cells (red) was observed not only in GFP$^-$ cells (PKA-ESCs) but also in GFP$^+$ cells (control ESCs); that is, considerable numbers of GFP$^+$Flk1$^+$ cells (white in Figure 1f) appeared from D2.5, suggesting faster differentiation of Control-ESCs in this condition. Flow cytometry analysis (Figures 1g and 1h) more clearly demonstrated the earlier and synchronized appearance of Flk1$^+$ cells after Dox depletion. In control condition (Dox+), both PKA-ESCs (blue dots) and Control ESCs (green dots) similarly differentiated into Flk1$^+$ cells at comparable levels until D4.5 (Figure 1g). In Dox- condition, which activates PKA only in PKA-ESCs, the appearance of Flk1$^+$ cells was evoked in PKA-ESCs from D2.5 and reached a much higher level at D3.5-4.5 than in control condition. As if following the earlier differentiation of PKA-ESCs, Flk1$^+$ cells in the Control-ESC population started to appear and eventually caught up in percentage with those in the PKA-ESC population by D3.5, even though Dox depletion did not activate PKA in Control-ESCs (Figure 1g). Consistently, the percentage of Flk1$^+$ cells in the Control-ESC population lagged behind that in the PKA-ESC population until D3.5, but their differentiation levels were synchronized thereafter (Figure 1h). A similar early and synchronized appearance of PDGFRα^+ cells in the Control-ESC population was seen in chimeric cell aggregates after PKA activation (Figures S2K-S2M). Together, these results indicate that there exists a novel cellular mechanism that synchronizes the cellular phenotypes of different cell populations (i.e., PSyC).

3.2 | PSyC is mediated by EVs

Next, we examined the mechanism of PSyC. We searched for intercellular communication systems that can conduct PSyC, such as humoral factors, gap junctions, and EVs, finding EVs as a potent candidate. EVs include exosomes and microvesicles (also called ectosomes). Exosomes are 50–150 nm-sized EVs that are generated by the inward budding of endosomes (Meldolesi, 2018). Microvesicles are 100–1000 nm-sized EVs that are generated by the direct budding of plasma membranes (Dang et al., 2013; Zhang et al., 2019). Cells transfer several types of biomolecules, including mRNAs, miRNAs and proteins, via EVs (Yáñez-Mó et al., 2015). We initially examined the loss-of-function of EVs by inhibiting EV secretion (Figure 2a). Manumycin A and GW4869 are two inhibitors of neutral sphingomyelinase 2 (nSMase2), an enzyme that regulates exosome secretion. Either manumycin A or GW4869 treatment specifically and significantly decreased the expression of Flk1$^+$ cells only in the Control-ESC population without affecting PKA-ESCs in chimeric aggregates under PKA activation at D3.5 (Figures 2b and 2c). Immunostaining revealed that the expression of Flk1 by Control-ESCs was decreased by the inhibitor treatment (Figure 2d, white). These results suggested the involvement of EVs in PSyC. To analyse the effect of EVs secreted from PKA-ESCs, we next isolated EVs in a conditioned medium of PKA-ESCs under non-active (EV (Dox+)) and active (EV (Dox-)) PKA conditions (Figure 2e). Immunoblotting confirmed the isolation of CD81-positive, flotillin1-positive and calnexin-negative EVs (Figure 2f). EVs were observed as vesicles 100–150 nm in diameter by electron microscopy and EV tracking analysis (Figures 2g, 2h and S3). The particle numbers and protein concentrations in EV (Dox+) and EV (Dox-) were not significantly different (Figures S4A and S4B). The addition of EV (Dox-) to pure Control-ESC aggregates induced a much higher percentage of Flk1$^+$ and PDGFRα^+ cells than no EVs or EV (Dox+) (Figures 2i, 2j, S4C and S4D). Consistently, immunostaining showed a dramatic increase in Flk1 and PDGFRα expression after EV (Dox-) treatment (Figure 2k). Additionally, PDGFRα-positive cells showed a tendency to increase dose-dependently (Figures S5A and S5B). These results indicate that EVs from activated PKA-ESCs enhance the differentiation of Control-ESCs to mesoderm to synchronize the differentiation levels.

Finally, we confirmed that PSyC was lost in a Transwell-mediated separated co-culture (Figure S6). This observation suggested that PSyC occurs only among cells in close proximity.

3.3 | EV-derived miRNAs regulate PSyC

Next, we tried to identify molecules within the EVs that induced PSyC. Global miRNA expression profiles contained in EV (Dox+) and EV (Dox-) were compared by RNA-seq (Figure 3a). We found that miR-126, -132, -184, -193a, -212 and -483 were enriched in EV (Dox-). We generated ESC lines overexpressing all 6 miRNA (multi-miR) or each miRNA together with GFP under a Dox-OFF system (Figure S7) and performed cell chimera experiments. The parental mouse ESC line (Era & Witte, 2000) for the miRNA-overexpressing cells does not carry any miRNA or GFP genes and was used as the recipient cells. In order to specifically evaluate the effects of miRNAs transferred from miRNA-expressing cells (GFP$^+$) to recipient cells (GFP$^-$), we analysed mesoderm induction only in recipient cells (Figure 3b). We generated chimeric cell aggregates with recipient cells and each miRNA-expressing cell line at a 1:3 ratio. Flk1$^+$ mesoderm differentiation in the recipient cells (GFP$^-$) was significantly promoted only when mixed with the miR-132 or multi-miR cell line (Figures 3b and 3c). We confirmed approximately 6-fold difference in the levels (counts per million) of miR-132 between EV (Dox+) and EV (Dox-) by RNA-seq (Figure S8). The copy number of miR-132 in the recipient cells was elevated after co-culture with PKA-ESCs (Figure S9). We also directly detected the transfer of PKA-ESC EV-derived miR-132 to the recipient cells by specific labelling with MB for miR-132 (Figure S10).

We further confirmed the role of EV-transferred miR-132 in the mesoderm induction of the recipient cells by generating miR-132 KO PKA-ESCs. EVs were prepared from the supernatants of PKA-ESCs or miR-132 KO PKA-ESCs after PKA activation

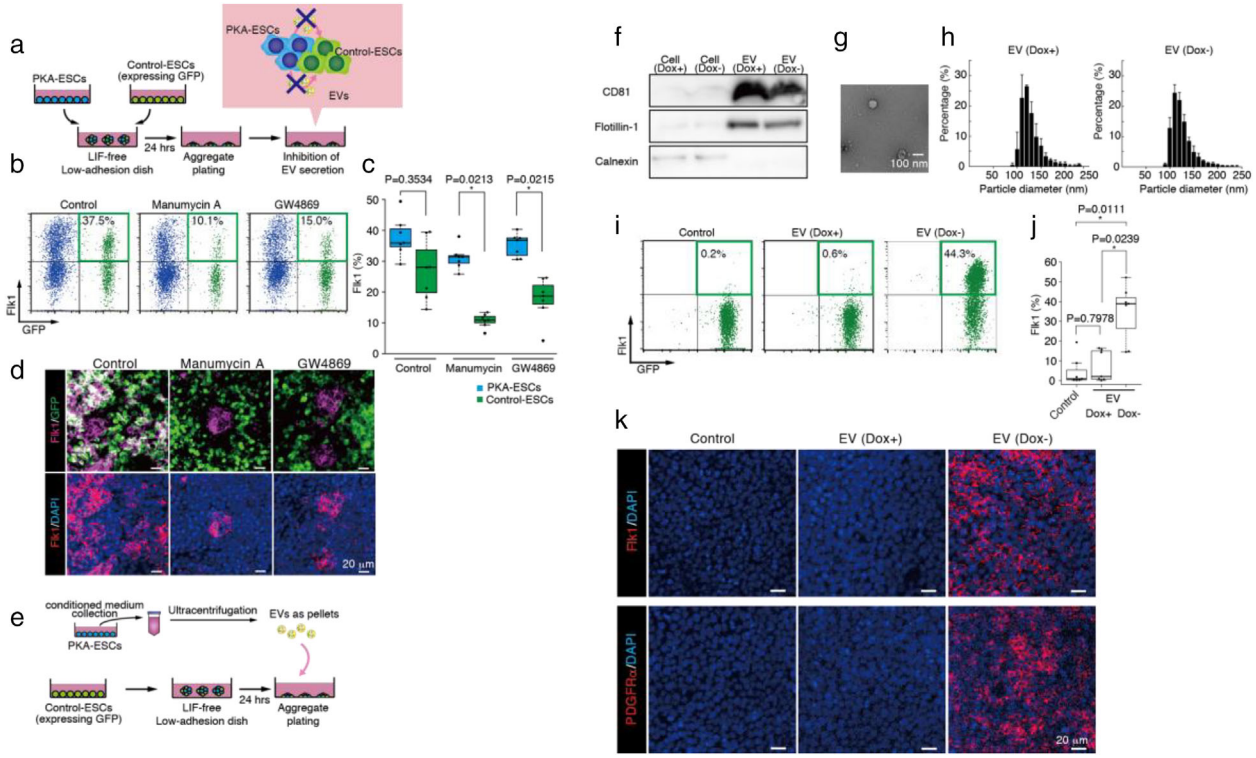

FIGURE 2 PSyC is mediated by EVs. (a) Schematic diagram of the chimeric aggregate co-culture differentiation system with EV secretion inhibited. PKA-ESCs and Control-ESCs were seeded in low adhesion dishes at a 3:1 ratio to create chimeric aggregates, and differentiation induction was initiated by the depletion of LIF. 24 h later, the aggregates were replated on normal plates and cultured with EV secretion inhibitors. (b) The number of Flk1$^+$ cells was reduced with treatment of the EV secretion inhibitors manumycin A (10 μM) or GW4869 (5 μM). PKA-ESC and Control-ESC chimeric aggregates on D3.5 under Dox- condition were analysed by FACS. (c) Percentage of PKA-ESCs and Control-ESCs in chimeric aggregates expressing Flk1 under Dox- condition. Data were analysed using the Kruskal-Wallis test followed by the Steel-Dwass test. (d) Immunostaining for Flk1$^+$ Control-ESCs (white) in chimeric aggregates with manumycin A (10 μM), GW4869 (5 μM), or DMSO (control). (e) Schematic diagram of the EV collection and treatment. Control-ESCs aggregates were plated without LIF. EVs were collected from the conditioned medium of PKA-ESCs as pellets and added to Control-ESCs aggregates. (f) Immunoblots of EV markers CD81 and Flotillin-1, non-EV marker calnexin in the cell or EV lysate (30 μg for CD81 and calnexin, 3 μg for Flotillin-1). (g) Transmission electron microscopy image of EVs from the conditioned medium. (h) Analysis of the EV size distribution in Dox+ (left) and Dox- (right) conditioned medium. (i) FACS analysis of Flk1$^+$ cells in EV-treated Control-ESCs on D3.5. (j) Percentage of Control-ESCs expressing Flk1. Data were analysed using the Kruskal-Wallis test followed by the Steel-Dwass test. (k) Immunostaining for mesodermal markers (Flk1, PDGFRα) in EV-treated Control-ESCs on D3.5

(Dox-) and added to the differentiating recipient cells. Whereas EV (Dox-) from PKA-ESCs enhanced the mesodermal differentiation of the recipient cells (similar to Figure 2i), EV (Dox-) from miR-132 KO PKA-ESCs (Dox-) failed to promote mesoderm differentiation (Figures S11A and S11B). When miR-132 expression was rescued in miR-132 KO PKA-ESCs, EVs could promote mesoderm differentiation (Figure S11B). These results indicate that miR-132 in EV (Dox-) is a major messenger molecule in the enhancement of mesoderm differentiation in recipient cells and contributes to PSyC.

We further examined the intracellular molecular machinery of the PSyC induction in recipient cells after they received EVs that carried miR-132. Spry1, an antagonist for fibroblast growth factor pathways, and Rasa1, a RasGAP activator, are targets of miR-132 (Dang et al., 2013; Gu et al., 2019; Lei et al., 2015). When Control-ESCs were treated with EV (Dox-), Spry1 and Rasa1 protein levels were significantly reduced, indicating that miR-132 acts in Control-ESCs through EV-mediated transfer (Figure 3d). miR-132 has been reported to activate Ras/Raf1 signalling by inhibiting Spry1 and Rasa1 (Lei et al., 2015). Additionally, Raf1 is reported to phosphorylate CREB via the adenylyl cyclase/cyclic AMP/PKA (Ding et al., 2004; Sassone-corsi, 2012) and ERK/RSK pathways (Mebratu & Tesfaigzi, 2009; Wang et al., 2018). Furthermore, pCREB upregulates the expression of ETS variant transcription factor 2 (ETV2) (Rasmussen et al., 2012) and Flk1 (Kataoka et al., 2011) genes, both of which are mesoderm inducers, and of miR-132 (Lin et al., 2012). Thus, the reduction of Spry1 and Rasa1 protein expression is postulated to activate PKA signalling through pCREB and result in mesoderm differentiation. Indeed, the levels of CREB phosphorylation (Figures 3d and 3e) and ETV2 mRNA (Figure 3f) in Control-ESCs were increased by the addition of EV (Dox-). Taken together, our results suggest a molecular link in PSyC after PKA activation as follows. First, PKA activation initiated in PKA-ESCs enhances Flk1$^+$ mesoderm cell differentiation as well as miR-132 expression through CREB phosphorylation. The activated PKA-ESCs then secrete EVs with high miR-132 content. miR-132 is delivered to the recipient cells via EV-mediated transfer and suppresses Spry1 and Rasa1, which in turn activates the PKA pathway through CREB phosphorylation in Control-ESCs. Thus, PKA activation initiated in the original PKA-ESCs can be reconstituted in Control-ESCs through PKA-ESC-derived EVs to evoke PSyC. Following these

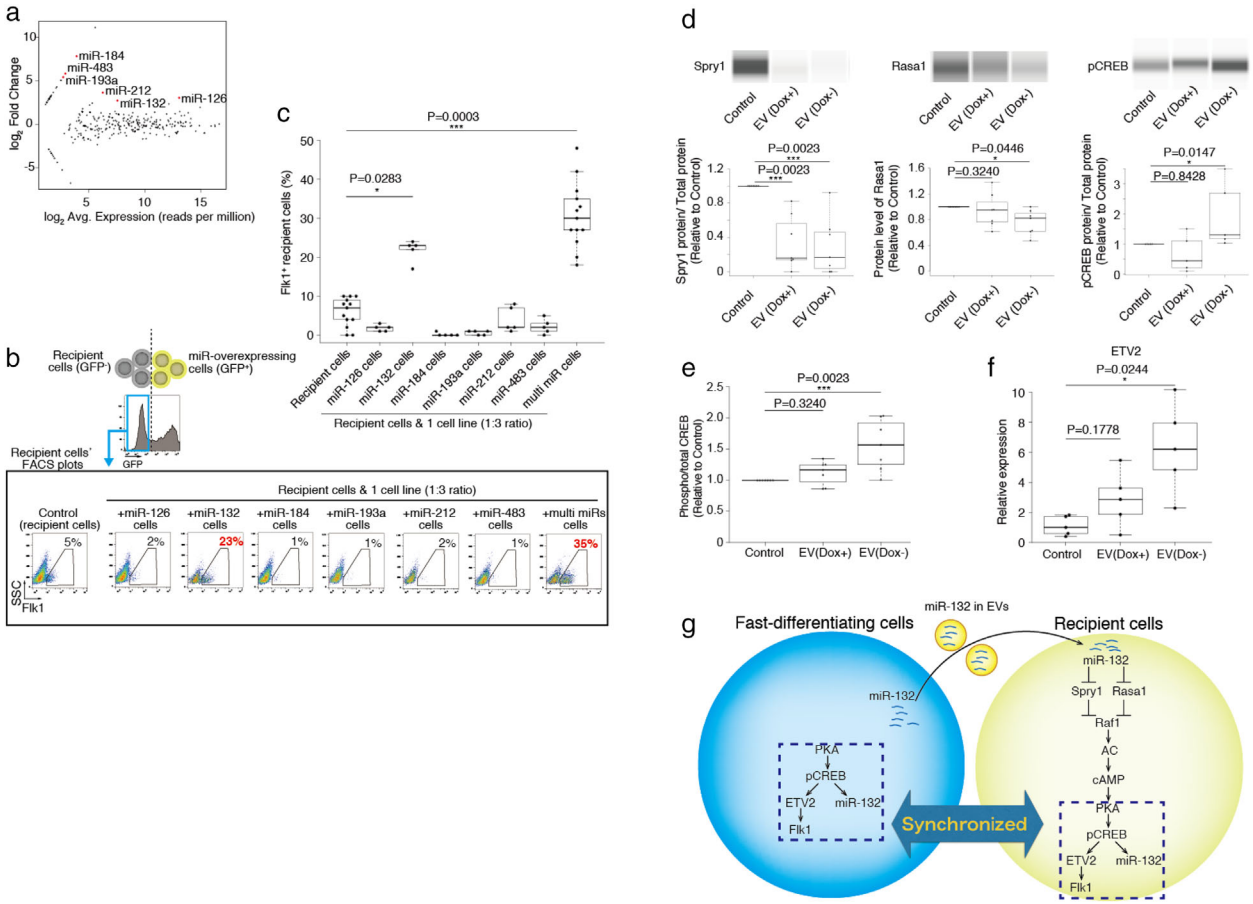

FIGURE 3 EV-derived microRNAs regulate PSyC. (a) An MA plot summarizing the differentially expressed miRNAs in EVs from activated PKA-ESCs (Dox-) versus EVs from inactivated PKA-ESCs (Dox+). (b) Flk1$^+$ recipient cells (EStTA5-4) in chimeric aggregates of recipient cells and miRNA-expressing cells (1:3 ratio). FACS plots showing recipient cells in chimeric aggregates with miRNA-expressing cell lines on D3.5. (c) Percentage of Flk1$^+$ recipient cells in aggregates at a 1:3 ratio. Data were analysed using the Kruskal-Wallis test followed by the Steel-Dwass test. (d) Detection of Spry1, Rasa1 and pCREB in capillary western blots. Proteins in the nuclear fractions were analysed to measure the expression levels of Spry1 and pCREB and normalized with Lamin A/C. Proteins in the cytoplasmic fractions were analysed to measure the expression level of Rasa1 and normalized with β-actin. Data were analysed using the Kruskal-Wallis test followed by the Steel-Dwass test. (e) pCREB and CREB levels were measured by ELISA. Data were analysed using the Kruskal-Wallis test followed by the Steel-Dwass test. (f) qPCR analysis of ETV2 in Control-ESCs treated with EVs from PKA-ESCs (Dox+ or Dox-) or without EVs. Data were analysed using the Kruskal-Wallis test followed by the Steel-Dwass test. (g) Schematic of the PSyC mechanism including EV secretion and miR-132 delivery. From fast-differentiating cells, miR-132 is passed through EVs to surrounding recipient cells, where it inhibits Spry1 and Rasa1 to transmit the signal. As a result, the differentiation mechanism is synchronized in the fast-differentiating cells and recipient cells

findings, we concluded that PSyC is a novel biological mechanism that reconstitutes similar intracellular environments in donor and recipient cells in close proximity via donor-derived EVs (Figure 3g).

3.4 | PKA-ESC EVs and miR-132 induce mesoderm and cardiac myocytes in mouse embryos

Finally, we examined whether EVs from differentiating ESCs affect cell fate during embryonic development. First, we tried to confirm the effect of EV (Dox-) on mesoderm-stage embryo. We collected E6.5 mouse embryos and cultured them ex vivo for 2 days with EV (Dox-) treatment (Figure 4a). We dissociated the embryos and examined PDGFRα^+ cells in the embryos after 2 days of ex vivo culture by FACS. Significantly more PDGFRα^+ cells were observed in the embryos when treated with EV (Dox-) compared to the untreated group (Figures 4b and 4c), suggesting that EV (Dox-) can enhance mesoderm differentiation in embryonic development.

We further examined the effects of EV (Dox-) on cell fate determination from an earlier stage of development. We applied a recently established ex vivo culture system for the observation of embryos continuously from the preimplantation to postimplantation stages (Bedzhov et al., 2014). We collected E3.5 mouse embryos and cultured them ex vivo with EVs (Figure 4d). Surprisingly, culturing the earlier embryos with EV (Dox-) drastically altered the embryo development. The appearance of cardiomyocytes with cardiac troponin-T-positive cells was enhanced in embryos treated with EV (Dox-) (five of 17 embryos), but

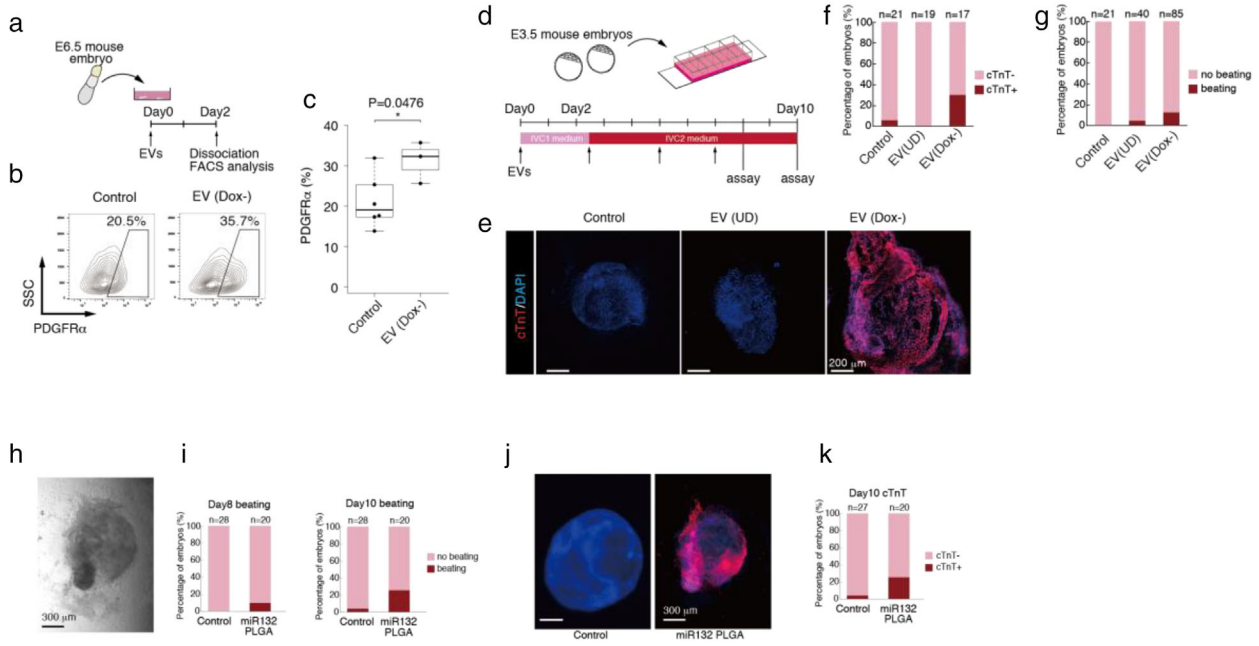

FIGURE 4 PKA-ESC-derived EVs and miR-132 induce mesoderm and cardiac myocytes in mouse embryos. (a) Schematic diagram of the mouse embryo culture. E6.5 mouse embryos were cultured for 2 days with EV treatment. At day 2, mouse embryos were dissociated and subjected to FACS analysis. (b) FACS analysis of PDGFRα expression on E6.5 embryos cultured for 2 days with EVs isolated from undifferentiated (UD) Control-ESCs or differentiating PKA-ESCs under Dox- condition. (c) Percentage of Control-ESCs expressing Flk1. Data were analysed using the Mann-Whitney U test. (d) Schematic diagram of the mouse embryo culture. E3.5 mouse embryos isolated from the uterus were cultured on μ slides in IVC1 medium. After attaching the mouse embryos to the slides on days 2–3, the medium was changed to IVC2 medium, and the embryos were cultured until day 8 or 10. EVs were added once every 2 days. (e) Immunostaining for cTnT on E3.5 mouse embryos cultured for 8 days with EVs isolated from UD Control-ESCs or differentiating PKA-ESCs under Dox- condition. (f and g) Percentage of $cTnT^+$ (f) and beating (g) embryos. E3.5 mouse embryos were cultured for 10 days with undifferentiated ESC-derived EVs (EV(UD)) or early differentiating PKA-ESC-derived EVs (EV(Dox-)). (h) A beating mouse embryo cultured for 10 days from E3.5 with miR-132-PLGA. (i) Percentage of beating embryos on day 8 and day 10. (j) Immunostaining for cTnT on E3.5 mouse embryos cultured for 10 days with or without miR-132-PLGA. (k) Percentage of $cTnT^+$ embryos on day 10

never in embryos treated with EVs collected from undifferentiated Control-ESCs (EV (UD)) (zero of 19 embryos) and rarely in untreated embryos (one of 21 embryos; Figures 4e and 4f). Additionally, whereas just weak beating or twitching was detected in only a few EV (UD)-treated and untreated embryos (two of 40 embryos and zero of 21 embryos, respectively), distinct cell clusters with apparent and typical spontaneous beating, sometimes dominating the whole embryo, were observed in EV (Dox-)-treated embryos (11 of 85 embryos; Figure 4g and Movie S1). Thus, EV (Dox-) has the potential to alter cell fate to mesoderm derivatives including cardiomyocytes in developing embryos.

We further confirmed whether miR-132 similarly works on cell fate determination. For this purpose, we employed an artificial polymeric nanoparticle, that is, formulated from biodegradable polymer poly (DL-lactide-co-glycolide) (PLGA) and can entrap various molecules including nucleic acids, penetrate cellular membranes, and deliver the encapsulated content into the cellular cytoplasm. We formulated PLGA nanoparticles containing miR-132 (miR-132-PLGA). miR-132-PLGA added to differentiating mouse ESCs successfully upregulated mesoderm marker Flk1 mRNA expression, indicating that miR-132-PLGA can mimic the function of EV (Dox-) (Figure S11C). When miR-132-PLGA was added to E3.5 mouse embryos, similar to that with EV (Dox-) addition, beating cardiomyocytes were observed from day 8 and increased in number until day 10. The percentage of embryos with beating cardiomyocytes was 3% in Control ($N = 28$) but as high as 25% in the miR-132-PLGA group ($N = 20$) (Figures 4h and 4i). All embryos with beating cardiomyocytes were positive for cardiac troponin-T (Figures 4j and 4k). Thus, we confirmed that miR-132 shows the same potential as EV (Dox-) with regards to altering cell fate towards mesoderm and cardiomyocytes in vivo.

4 | DISCUSSION

Here we showed a novel biological phenomenon in which cellular phenotypes are synchronized during differentiation by a type of EV-mediated cell-cell communication we call 'Phenotypic Synchrony of Cells (PSyC)'. We identified one potential candidate molecule in the EVs, miR-132, that can reconstitute the molecular link in the recipient cells for PSyC and reproduce the in vivo effects of EVs to induce mesoderm derivatives.

Though various mesoderm-inducing molecules have been reported previously, such as basic fibroblast growth factor (bFGF), bone morphogenetic protein (BMP), and PKA pathway molecules, our global protein analysis with mass spectrometry showed that these molecules were not enriched in EV (Dox-) (data not shown). Instead, miR-132, which has not been previously reported to induce mesoderm, was enriched and could evoke mesoderm induction in EV-recipient cells through the reconstitution of PKA activation. Specifically, we found that miR-132-PLGA promotes mesoderm differentiation in ESCs and induces beating cardiomyocytes in mouse embryos (Figures S11C and 4h-k), indicating that miR-132 alone can induce mesoderm lineages to some degree. However, considering that EVs contain thousands of biomolecules, such as miRNAs and proteins, the observed miR-132-mediated effect should represent only part of the EV-mediated PSyC mechanism. Even in EVs from miR-132-overexpressing cells, other EV molecules may have contributed to the PSyC mechanism. Moreover, PSyC may more broadly contribute to cell and tissue development and homeostasis. The PSyC phenomenon we demonstrated here would be just one type of PSyC effect. We speculate that the molecules responsible for PSyC vary with the cell type and microenvironment. For example, it has been reported that Cav1 KO adipocytes receive Cav1 mRNA from surrounding endothelial cells via EVs, allowing the KO cells to produce Cav1 protein (Crewe et al., 2018). Another report suggested the involvement of EVs in homeostasis, in which ESC-derived EVs maintain the stem cell properties of ESCs even under differentiation culture conditions (Hur et al., 2021). Accordingly, PSyC with different conditions and environments should be investigated.

Recently, EVs were highlighted as a novel cell-cell communication modality that acts through remote effects analogous to hormones (Zhang et al., 2019). On the contrary, in PSyC, EVs function at short-range, transmitting the cellular state to surrounding cells in cell aggregates. This synchronizing effect was largely reduced when PKA-ESCs and Control-ESCs were separately cultured by applying a Transwell membrane (Figure S6), suggesting that the EVs are absorbed by neighbouring cells to exert PSyC. Such results were supported by a second experiment. When ESCs releasing tdTomato-labelled EVs were co-cultured with Control-ESCs, only little EVs were observed when the cells were separately cultured with Transwells. In contrast, much more EVs were observed in mixed aggregation conditions (Figure S12). Thus, PSyC can regulate cells by a new-mode EV function directly transferring EVs to neighbouring cells.

EVs are a heterogeneous group of cell-derived membranous structures including exosomes and microvesicles, which originate from the endosomal system or which are shed from the plasma membrane, respectively (van Niel et al., 2018). Exosomes are generated by endosomal sorting complex required for transport (ESCRT)-dependent and ESCRT-independent mechanisms (van Niel et al., 2018). It has been reported that the silencing of tumour susceptibility gene 101 (TSG101), a component of the ESCRT complex, reduces exosome secretion (Hessvik & Llorente, 2018; Riva et al., 2019). The generation of arrestin domain containing 1 (ARRDC1)-mediated microvesicles also requires TSG101 (Nabhan et al., 2012). Consistently, it has been reported that TSG101 KO inhibits cell proliferation and differentiation, and TSG101 KO mice show embryonic lethality around the implantation stage (Wagner et al., 2003). In contrast, mice knocked out of nSMase2, which is involved in ESCRT-independent exosome production, show hypoplasia and growth retardation in all tissues, but no fetal lethality (Stoffel et al., 2005). It has been suggested that miRNA-containing EVs are preferentially produced via the SMase2/ceramide pathway, which is distinct from the canonical ESCRT pathway (Record et al., 2018). In our study, PSyC was significantly but not completely blocked by nSMase2 inhibitors (Figures 2b and 2c). We further confirmed that the copy number of miR-132 was reduced by approximately 20 to 70 % in EVs after nSMase2 was inhibited by the addition of manumycin A (Figure S13). These results suggest the involvement of ESCRT-independent pathways but also of other EV generation mechanisms, ESCRT-dependent exosomes and/or microvesicles in PSyC.

Though EVs from PKA-ESCs caused a dose-dependent increase of PDGFRα-positive cells in Control-ESCs (Figures S5A and S5B), high doses reduced the number of Flk1-positive cells (Figures S5C and S5D). Flk1 and PDGFRα represent overlapping but distinct subsets of mesoderm, lateral plate mesoderm (LPM) and para-axial mesoderm (PAM), respectively (Kataoka et al., 1997). Though PKA-ESC EVs apparently increased both cell populations, the effects became opposite for Flk1-positive cell appearance only in higher doses, suggesting that PKA-ESC EVs basically possess the synchronization potentials to mesoderm broadly, but there may exist further fine-tuned synchronization potential to a specific subset of mesoderm. If so, PKA-ESC EVs are likely more suitable for the synchronization to PAM than LPM.

To conclude, we report a new intercellular communication mechanism between cells in close proximity. Different from several reports that found EVs influence the differentiation of specific cell types (Yáñez-Mó et al., 2015), we speculate that PSyC can establish cell subsets to build normal tissues through a synchronization mechanism that closely aligns cell fate determination and differentiation stages. Further, PSyC could be a critical mechanism for broadly regulating tissue development and homeostasis, as tissues and organs may be established and maintained by the fine-tuned molecular transport of EV among neighbouring cells, a phenomenon not highlighted before. Advanced imaging of EV function and behaviour could directly demonstrate the dynamics of cell-cell communications.

4.1 | Limitations

EVs contain thousands of non-coding RNAs and hundreds of proteins that engage in number of signalling pathways and gene networks. However, in this study, we only focused our analysis on miRNAs, especially miR-132.

ACKNOWLEDGEMENTS

We thank Dr. T. Matsunaga and T. Hoshino for technical suggestions; Dr. P. Karagiannis for critical reading of the manuscript; Dr. A. Watanabe, Dr. M. Nakamura and N. Amano for analysing the RNA-seq data; Dr. Takumi Era for providing the EStTA5-4 cell line, Dr. Feng Zhang for providing the pX330 plasmid and Dr. Knut Woltjen for providing the piggyBac vector and transposon vector; Dr. I. Baba, Kozue Nakamura, Kae Nakamura, Y. Kaji and N. Yasuhara for technical assistance; and Dr. M. Kengaku and ZEISS-iCeMS Innovation Core at the iCeMS Analysis Centre, Kyoto University, for supporting the imaging analysis. This work was supported by JST CREST Grant Number JPMJCR17H5, Japan.

AUTHOR CONTRIBUTIONS

T. Minakawa and J.K.Y. designed the experiments. T. Minakawa performed the experiments including the cell culture, FACS, qRT-PCR, immunostaining, EV collection, EV analysis and mouse embryo culture. T. Matoba prepared the PLGA nanoparticles. F.I. and T.K.F. supported the imaging analysis. Y.T. and S.T. prepared the MB and the cationized gelatin nanospheres. T. Minakawa and J.K.Y. wrote the manuscript. J.K.Y. supervised the study.

ORCID

Tomohiro Minakawa https://orcid.org/0000-0002-6754-6337
Jun K. Yamashita https://orcid.org/0000-0002-8460-0665

REFERENCES

Arnold, S. J., & Robertson, E. J. (2009). Making a commitment: Cell lineage allocation and axis patterning in the early mouse embryo. *Nature Reviews Molecular Cell Biology 10*, 91–103.

Bedzhov, I., Leung, C., Bialecka, M., & Zernicka-Goetz, M. (2014). In vitro culture of mouse blastocysts beyond the implantation stages. *Nature Protocols*, *9*, 2732–2739.

Chevillet, J. R., Kang, Q., Ruf, I. K., Briggs, H. A., Vojtech, L. N., Hughes, S. M., Cheng, H. H., Arroyo, J. D., Meredith, E. K., Gallichotte, E. N., Pogosova-Agadjanyan, E. L., Morrissey, C., Stirewalt, D. L., Hladik, F., Yu, E. Y., Higano, C. S., & Tewari, M. (2014). Quantitative and stoichiometric analysis of the microRNA content of exosomes. *Proceedings National Academy of Science USA 111*, 14888–14893.

Crewe, C., Joffin, N., Rutkowski, J. M., Kim, M., Zhang, F., Towler, D. A., Gordillo, R., & Scherer, P. (2018). An endothelial-to-adipocyte extracellular vesicle axis governed by metabolic state. *Cell 175*, 695–708.

Dang, L. T. H., Lawson, N. D., & Fish, J. E. (2013). MicroRNA control of vascular endothelial growth factor signaling output during vascular development. *Arteriosclerosis, Thrombosis, and Vascular Biology 33*, 193–200.

Ding, Q., Gros, R., Gray, I. D., Taussig, R., Ferguson, S. S. G., & Feldman, R. D. (2004). Raf kinase activation of adenylyl cyclases: Isoform-selective regulation. *Molecular Pharmacology 66*, 921–928.

Era, T., & Witte, O. (2000). Regulated expression of P210 Bcr-Abl during embryonic stem cell differentiation stimulates multipotential progenitor expansion and myeloid cell fate. *Proceedings of the National Academy of Sciences of the United States of America 97*, 1737–1742.

Evans, M. J., & Kaufman, M. H. (1981). Establishment in culture of pluripotential cells from mouse embryos. *Nature 292*, 154–156.

Gu, X., Su, X., Jia, C., Lin, L., Liu, S., Zhang, P., Wang, X., & Jiang, X. (2019). Sprouty1 regulates neuritogenesis and survival of cortical neurons. *Journal of Cellular Physiology 234*, 12847–12864.

Hessvik, N. P., & Llorente, A. (2018). Current knowledge on exosome biogenesis and release. *Cellular and molecular life sciences : CMLS 75*, 193–208.

Hur, Y. H., Feng, S., Wilson, K. F., Cerione, R. A., & Antonyak, M. A. (2021). Embryonic stem cell-derived extracellular vesicles maintain ESC stemness by activating FAK. *Developmental Cell 56*, 277–291.

Kataoka, H., Hayashi, M., Nakagawa, R., Tanaka, Y., Izumi, N., Nishikawa, S., Jakt, M. L., Tarui, H., & Nishikawa, S. I. (2011). Etv2 /ER71 induces vascular mesoderm from Flk1^{+}PDGFRα^{+} primitive mesoderm. *Blood 118*, 6975–6986.

Kataoka, H., Takaura, N., Nishikawa, S., Tsuchida, K., Kodama, H., Kunisada, T., Risau, W., Kita, T., & Nishikawa, S. I. (1997). Expressions of PDGF receptor alpha, c-Kit and Flk1 genes clustering in mouse chromosome 5 define distinct subsets of nascent mesodermal cells. *Development, Growth & Differentiation 39*, 729–740.

Kawashima, Y., Yamamoto, H., Takeuchi, H., Hino, T., & Niwa, T. (1998). Properties of a peptide containing DL-lactide/glycolide copolymer nanospheres prepared by novel emulsion solvent diffusion methods. *European Journal of Pharmaceutics and Biopharmaceutics 45*, 41–48.

Lei, Z., Mil, A. V., Brandt, M. M., Grundmann, S., Hoefer, I., Smits, M., Azzouzi, H. E., Fukao, T., Cheng, C., Doevendans, P. A., & Sluijter, J. P. (2015). MicroRNA-132/212 family enhances arteriogenesis after hindlimb ischaemia through modulation of the Ras-MAPK pathway. *Journal of Cellular and Molecular Medicine 19*, 1994–2005.

Lin, L., Chiu, S., Wu, M., Chen, P., & Yen, J. (2012). Luteolin induces microRNA-132 expression and modulates neurite outgrowth in PC12 cells. *Plos One 7*, e43304.

Martin, G. R. (1981). Isolation of a pluripotent cell line from early mouse embryos cultured in medium conditioned by teratocarcinoma stem cells. *Proceedings of the National Academy of Sciences of the United States of America 78*, 7634–7638.

Mebratu, Y., & Tesfaigzi, Y. (2009). How ERK1/2 activation controls cell proliferation and cell death is subcellular localization the answer ? *Cell Cycle 8*, 1168–1175.

Meldolesi, J. (2018). Exosomes and ectosomes in intercellular communication. *Current Biology 28*, R435–R444.

Minakawa, T., Kanki, Y., Nakamura, K.&, Yamashita, J. K. (2020). Protein kinase A accelerates the rate of early stage differentiation of pluripotent stem cells. *Biochemical and Biophysical Research Communications 524*, 57–63.

Murata, Y., Jo, J. I., & Tabata, Y. (2021). Molecular beacon imaging to visualize Ki67 mRNA for cell proliferation ability. *Tissue Engineering. Part A 27*, 526–535.

Nabhan, J. F., Hu, R., Oh, R. S., Cohen, S. N., & Lu, Q. (2012). Formation and release of arrestin domain-containing protein 1-mediated microvesicles (ARMMs) at plasma membrane by recruitment of TSG101 protein. *Proceedings of the National Academy of Sciences of the United States of America 109*, 4146–4151.

Rasmussen, T. L., Shi, X., Wallis, A., Kweon, J., Zirbes, K. M., Koyano-Nakagawa, N., & Garry, D. J. (2012). VEGF /Flk1 signaling cascade transactivates Etv2 gene expression. *Plos One 7*, e50103.

Record, M., Silvente-Poirot, S., Poirot, M., & Wakelam, M. J. O. (2018). Extracellular vesicles: Lipids as key components of their biogenesis and functions. *Journal of Lipid Research 59*, 1316–1324.

Riva, P., Battaglia, C., & Venturin, M. (2019). Emerging role of genetic alterations affecting exosome biology in neurodegenerative diseases. *International Journal of Molecular Sciences 20*, 4113.

Sassone-corsi, P. (2012). The cyclic AMP pathway. *Cold Spring Harbor perspectives in biology 4*, a011148.

Stoffel, W., Jenke, B., Blöck, B., Zumbansen, M., & Koebke, J. (2005). Neutral sphingomyelinase 2 (smpd3) in the control of postnatal growth and development. *Proceedings of the National Academy of Sciences of the United States of America 102*, 4554–4559.

Thomson, J. A., Itskovits-Eldor, J., Shapiro, S. S., Waknitz, M. A., Swiergial, J. J., Marshall, V. S., & Jones, J. M. (1998). Embryonic stem cell lines derived from human blastocysts. *Science 282*, 1145–1148.

van Niel, G., D'Angelo, G., & Raposo, G. (2018). Shedding light on the cell biology of extracellular vesicles. *Nature Reviews Molecular Cell Biology 19*, 213–228.

Wagner, K. U., Krempler, A., Qi, Y., Park, K., Henry, M. D., Triplett, A. A., Riedlinger, G., Rucker, E. B. III, & Hennighausen, L. (2003). Tsg101 is essential for cell growth, proliferation, and cell survival of embryonic and adult tissues. *Molecular and Cellular Biology 23*, 150–162.

Wang, H., Xu, J., Lazarovici, P., Quirion, R., & Zheng, W. (2018). cAMP response element-binding protein (CREB): A possible signaling molecule link in the pathophysiology of schizophrenia. *Frontiers in molecular neuroscience 11*, 255.

Woltjen, K., Michael, I. P., Mohseni, P., Desai, R., Mileikovsky, M., Hämäläinen, R., Cowling, R., Wang, W., Liu, P., Gertsenstein, M., Kaji, K., Sung, H. K., & Nagy, A. (2009). piggyBac transposition reprograms fibroblasts to induced pluripotent stem cells. *Nature 458*, 766–770.

Yamamizu, K., Kawasaki, K., Katayama, S., Watabe, T., & Yamashita, J. K. (2009). Enhancement of vascular progenitor potential by protein kinase A through dual induction of Flk-1 and Neuropilin-1. *Blood 114*, 3707–3716.

Yamashita, J., Itoh, H., Hirashima, M., Ogawa, M., Nishikawa, S., Yurugi, T., Naito, M., Nakao, K., & Nishikawa, S. (2000). Flk1-positive cells derived from embryonic stem cells serve as vascular progenitors. *Nature 408*, 92–96.

Yáñez-Mó, M., Sijander, P. R-M., Andreu, Z., Zavec, A. B., Borràs, F. E., Buzas, E. I., Buzas, K., Casal, E., Cappello, F., Carvalho, J., Colás, E., Cordeiro-da Silva, A., Fais, S., Falcon-Perez, J. M., Ghobrial, I. M., Giebel, B., Gimona, M., Graner, M., Gursel, I.…De Wever, O. (2015). Biological properties of extracellular vesicles and their physiological functions. *Journal of extracellular vesicles 4*, 27066.

Yurugi-Konayashi, T., Itoh, H., Schroeder, T., Nakano, A., Narazaki, G., Kita, F., Yanagi, K., Hiraoka-Kanie, M., Inoue, E., Ara, T., Nagasawa, T., Just, U., Nakao, K., Nishikawa, S., & Yamashita, J. K. (2006). Adrenomedullin/cyclic AMP pathway induces Notch activation and differentiation of arterial endothelial cells from vascular progenitors. *Arteriosclerosis, Thrombosis, and Vascular Biology 26*, 1977–1984.

Zhang, Y., Liu, Y., Liu, H., & Tang, W. H. (2019). Exosomes: Biogenesis, biologic function and clinical potential. *Cell & bioscience 9*: 19.

SUPPORTING INFORMATION

Additional supporting information may be found in the online version of the article at the publisher's website.

How to cite this article: Minakawa, T., Matoba, T., Ishidate, F., Fujiwara, T. K., Takehana, S., Tabata, Y., & Yamashita, J. K. (2021). Extracellular vesicles synchronize cellular phenotypes of differentiating cells. *Journal of Extracellular Vesicles*, *10*, e12147. https://doi.org/10.1002/jev2.12147